Salt Tectonics and its Effect on Sediment Structure and Gas Hydrate Occurrence in the Northwestern Gulf of Mexico from 2D Multichannel Seismic Data

Dan'l Lewis and William Sager

Department of Oceanography, Texas A&M University, MS 3146, College Station, Texas 77843–3146, U.S.A.

ABSTRACT

This study was undertaken to investigate mobile salt and its effect on fault structures and gas hydrate occurrence in the northwestern Gulf of Mexico. Industry 2D multichannel seismic data were used to investigate the effects of salt within an area of 7577 mi^2 (19,825 km^2) on the Texas continental slope in the northwestern Gulf of Mexico. The western half of the study area is characterized by a thick sedimentary wedge and isolated salt diapirs whereas the eastern half is characterized by a massive and nearly continuous salt sheet topped by a thin sedimentary section. This difference in salt characteristics marks the edge of the continuous salt sheets of the central Gulf of Mexico and is likely a result of westward decline of original salt volume. Beneath the sedimentary wedge in the western part of the survey, an anomalous sedimentary package was found, that is described here as the diapiric, gassy sediment package (DGSP). The DGSP is highly folded at the top and is marked by tall, diapiric features. It may be either deformed shale or the toe of a complex thrust zone detaching the sedimentary wedge from deeper layers. The dataset was searched for the occurrence of bottom simulating reflectors (BSRs) because they are widely accepted as a geophysical indicator of gas trapped beneath gas hydrate deposits that are known to occur farther east in the Gulf. Although, many seismic signatures were found that suggest widespread occurrence of gas within the upper sediment column, few BSRs were found. Even considering non-traditional definitions of BSRs, only a few occurrences of patchy and isolated BSRs features were identified. The lack of traditional BSRs is likely the result of geologic conditions that make it difficult to recognize gas hydrate deposits. These factors include: (1) unfavorable layer geometries, (2) flow of warm brines from depth, (3) elevated geotherms due to the thermogenic properties of salt and its varying thickness, and (4) widespread low porosity and permeability sediments within the gas hydrate stability zone.

INTRODUCTION

Despite being a passive continental margin, the Texas continental slope of the northern Gulf of Mexico is tectonically active and complex owing to mobile salt (Pindell, 1985; Worrall and Snelson, 1989; Salvador, 1991). Tectonic complexity is evident from the rugged bathymetry of the Gulf of Mexico seafloor (Bryant et al., 1990) (Fig. 1), a result of a great wedge of sediments mobilizing buried salt to ascend through the sediment column. Our region of interest, the Texas slope, is also affected by

mobile shale bodies that further complicate the subsurface structure (Bruce, 1973; Bishop, 1977; Camerlo et al., 2004). The Texas slope appears to be a transitional area because the bathymetry displays a shift from the rugged seafloor of the Louisiana slope to the smoother seafloor of the Texas slope. The Texas slope is also narrower than the Louisiana slope apparently because of less extensive sediment accumulation and basinward motion of salt sheets. In the western Gulf of Mexico there is also a transition from an area including the northern Mexico continental slope, where gas hydrate accumulation is indicated by a bottom-simulating reflectors (BSRs) (Krason et al., 1985) to a region where gas hydrate is common (MacDonald et al., 1994), but BSRs occur only rarely, as on the Louisiana continental slope (Shedd et al., 2012). Recent studies suggest that BSRs in the northern Gulf of Mexico do indeed occur, but they are complex in nature and mostly do not have the characteristics that normally

define a BSR (i.e., a continuous reflector that mimics the seafloor and cross-cuts sedimentary strata) (Shedd et al., 2009, 2012). MacDonald et al. (1994) suggested the Texas slope was less prone to hydrocarbon seeps, which could indicate a reduced free gas volume for the area.

While geophysical exploration in the northwest Gulf of Mexico, overall, is high, there have been relatively few published geophysical studies of the Texas slope. This limited information not only applies to the subsurface, but also to the seafloor, where high-resolution bathymetry, which has been published for most of the Gulf, is not available. The motivation for this project comes from access to a large, regional 2D multi-channel seismic (MCS) grid that allows us to explore broad differences in structural features, such as the top of salt and faulting. Further, this seismic analysis helped achieve a better understanding of seafloor morphology, implications of tectonic processes, and evaluation of the area for the geophysical indicators of both gas and gas hydrates, which are known to occur in the area (MacDonald et al., 2003; McConnell and Kendall, 2003; Frye, 2008; Shedd et al., 2009, 2012).

BACKGROUND

Gulf of Mexico History

The present day Gulf of Mexico is considered a passive continental margin, but its current form is the product of multiple rifting episodes, crustal extension, large volumes of sediment accumulation, and salt emplacement and mobilization (Worrall and Snelson, 1989; Salvador, 1991). Rifting in the Late Triassic to Early Jurassic resulted in the formation of graben and half-graben into which salt began to deposit in the Middle to Late Jurassic (Salvador, 1991; Sawyer et al., 1991; Watkins et al., 1995). Salt deposits were thickest in the graben, as they had a larger accommodation space, and thinnest over structural highs and the landward edge of the basin (Watkins et al., 1995). The thickness distribution of the salt suggests that some of the graben systems remained active throughout the Middle Jurassic and possibly into the Late Jurassic, whereas other areas may represent younger rifting and subsidence (Salvador, 1991). Marine sediments began to deposit in the basin over the salt layer, which began the process of sediment loading and deformation that continues through today (Galloway, 1989; Worrall and Snelson, 1989; Salvador, 1991).

Sedimentation has occurred almost continuously in the Gulf of Mexico since the deposition of the salt, punctuated only by occasional hiatuses that are seen typically at the basin edge (Salvador, 1991). Sedimentation on the Texas slope in the Cretaceous and into the early Cenozoic was dominated by Texas river systems, which led to the deposition of a thick, sedimentary wedge, overlying malleable salt (Worrall and Snelson, 1989). By the mid-Cenozoic, northern Gulf of Mexico sedimentation had shifted mainly to the east, and was controlled mostly by the Mississippi River and its ancestral rivers, a situation that has continued into the present day (Galloway, 1989; Salvador, 1991). As the massive Cenozoic sediment wedge was deposited, its weight caused the buried salt to mobilize and form allochthonous salt sheets that moved upsection into the shallow subsurface. Rowan et al. (2004) suggested that an abundance of salt and the early triggering of deformation beneath a thin overburden resulted in the occurrence of diapirs. However, south of the Texas slope where the Perdido fold belt occurs, Rowan et al. (2004) explained that a lack of early deformation was responsible for the absence of diapirs and the relative simplicity of the Perdido fold belt rela-

tive to fold belts farther east. Later sedimentation drove massive salt mobilization synchronously with gravity-driven sliding of salt and sediments toward the center of the basin. These two processes gave rise to two dominating styles of faulting: Texas-style and Louisiana-style faults (Worrall and Snelson, 1989). Texas-style faults are long, listric and are indicative of subsidence of sediment and gravitational sliding. In contrast, Louisiana-style faults are shorter and are typically related to a thin sedimentary section and shallow salt structure where they typically sole into the top of the salt canopy and thus are directly related to salt tectonism (Worrall and Snelson, 1989).

Gas Hydrates and BSRs

Gas hydrates are known to occur in the northern Gulf of Mexico; however, their extent and volume are still uncertain. Frye (2008) concluded that gas hydrate exists in large volumes across the entire Gulf region, based on a gas hydrate stability zone modeled after Milkov and Sassen (2001) and statistical estimates of factors affecting gas hydrate occurrence. Gas hydrates have been confirmed by the DOE/Joint Industry Project Leg I and Leg II drilling (Ruppel et al., 2008; Boswell et al., 2009, 2012), as well as with photographic evidence (MacDonald et al., 1994). However, there is little seismic evidence in the region for traditional BSRs, a widely-used indicator of gas hydrate occurrence. As originally defined, a BSR is continuous reflector that mimics the shape of the seafloor and crosscuts sedimentary strata (Shipley et al., 1979; Dillon and Paull, 1983; Dillon et al., 1996). They occur at the base of the gas hydrate stability zone (BGHSZ) where free gas pools as it is prevented from moving upward by sediment porosity filled with gas hydrate. This gas-rich layer causes a drop in sonic velocity, which causes the acoustic contrast that results in a BSR. Owing to the decrease in velocity, BSRs in seismic sections produce a polarity reversal (Kvenvolden, 1993). The BSR is often accompanied by seismic "blanking," a zone above the BSR where seismic stratigraphy is muted owing to the reduction of seismic impedance contrast by gas hydrate fill (Hornbach et al., 2003; Riedel et al., 2005).

Recent studies of the seismic signature of gas hydrate in the northern Gulf of Mexico have stretched the definition of BSRs because the traditional model is mainly applicable to regions with structurally simple homogenous sediment layers, whereas northern Gulf of Mexico sediments vary greatly in porosity and permeability (McConnell and Kendall, 2003) and have complex stratal structures. Regions like the Gulf of Mexico with heterogeneous sediment layers and significant structure may have a BGHSZ that is irregular in nature due to lateral variations in porosity and permeability. In the Gulf of Mexico, the sedimentary column often contains fine-grained sediments (compacted clay, mud, and silt) with low porosity interbedded with coarse-grained sands with high porosity and permeability. Gas can accumulate in significant amounts to form high volume gas hydrate deposits only in the coarse sediments or fractures within the fine-grained sediments (Boswell and Collett, 2011; Boswell et al., 2012).

The geothermal gradient in shallow regions (<3000 ft [<1000 m]) can also be perturbed due to long term climate change, complex geologic structure, and fluid movement (Nagihara, 2006). This lateral variability gives rise to gas reflectors that no longer mimic seafloor shape, but are still termed BSR because they are caused by an analogous process. The expanded definition of BSRs includes continuous, discontinuous and "high-relief" or "plume" (Shedd et al., 2009, 2012). These types are defined as follows: (1) a continuous BSR is a continuous reflector with negative polarity and clear cross-cutting of strata; (2) a

"discontinuous BSR" is formed by discrete seismic anomalies (bright spots and phase reversals) occurring in porous sediment layers with the bright spots aligning along the predicted BGHSZ; and (3) a "high-relief" or "plume BSR" does not mimic the seafloor, but it represents locations where the BGHSZ is perturbed upward by local variations in thermal gradient related to salt structure and fluid flow. Work by Shedd et al. (2009, 2012) showed that discontinuous BSRs are the most common form in the Gulf of Mexico and are typically located along the flanks and centers of mini-basins. Shedd et al. (2009, 2012) interpret these as locations where the BGHSZ cross-cuts sedimentary sections consisting of interbedded sands and shales, in which the bright spots are created within sand-rich units and separated by fine grained units containing little or no gas hydrate. High-relief BSRs are the least common and can incorporate features that are both continuous and discontinuous (Shedd et al., 2009, 2012). High-relief BSRs are interpreted to mark the BGHSZ in areas prone to laterally variable heat flow, especially over salt bodies where vertically migrating gas, oil, and warm brine cause the hydrate stability zone to thin dramatically (Ranganathan and Hanor, 1988; Petersen and Lerche, 1996; Shedd et al., 2009, 2012).

METHODS/DATA

This study examined a large industry 2D multichannel seismic (MCS) dataset collected by TGS-NOPEC, Inc. These data were collected from November 7, 1988, to November 7, 1989, and cover a large area (7577 mi^2 [19,625 km^2]) of the upper Texas continental slope (Fig. 1). Processing was completed in April 1990 by Digicon Geophysical Corporation. The area covered by the dataset encompasses two main outer continental shelf (OCS) protraction zones: East Breaks and Corpus Christi. The dataset also overlaps surrounding protraction areas: Port Isabel, Alaminos Canyon, Keathley Canyon, Garden Banks, High Island East Addition South Extension, High Island South Addition, Galveston South Addition, Brazos South Addition, Mustang Island East Addition, and North Padre Island East Addition (Fig. 2). Seismic sections are limited to 0 to 6.7 s two-way travel time (TWTT). The survey used a hydrophone array (streamer) with 240 channels and a length of ~20,000 ft (6000 m). The survey was done in two parts with the western half having ~6 mi (10 km) grid spacing and the eastern half having ~2 mi (3.3 km) grid spacing (Fig. 2). The shotpoint interval in both areas is 164 ft (50 m) and the group interval is 82 ft (25 m) and the nominal fold is 60. Data in the two areas were sampled at 4 ms for the coarse, western part of the survey and 1 ms for the tighter grid of the eastern survey. The processing sequence included spherical divergence correction, exponential gain correction, deconvolution, and normal moveout correction, as well as dip moveout velocity analysis every mile and a 60-fold dip moveout stack. Noise suppression, a time varying filter, and a relative amplitude scaling were applied to time migrated data.

Seismic interpretation was done using Kingdom Suite software version 8.5 by Seismic Micro-Technology, Inc. Top of salt (TOS) was picked as a horizon across the study area. TOS was identified by a strong acoustic impedance contrast overlying an acoustically chaotic zone with little evidence of internal seismic reflections. An additional criterion for picking TOS was the occurrence of acoustic reverberation, which we define as a zone of enhanced return with a lack of internal structure, below strong acoustic impedance reflectors. In addition, structural deformation around the TOS was taken as an indication that the reflector was caused by mobile salt.

Faults were identified as terminations of beds, offset of strata and seafloor, as well as aligned breaks (diffraction) of seismic layering. Gas indicators were mapped across the region as horizons where they were nearly horizontal and continuous and were indicated by bright spots or sections of low internal reflectivity (acoustic blanking). Disseminated free gas was interpreted by acoustic turbidity or acoustic wipeout signatures. Potential BSR candidates were mapped as a horizon as long as they met all of the following criteria: (1) they were bright spots or a sequence of bright spots with crosscutting relationships with surrounding strata; (2) they mimic the seafloor; (3) they occur within the modeled BGHSZ range for 90.4–100% methane (Milkov and Sassen, 2001); (4) they showed a signal phase inversion relative to the seafloor on at least a portion of the horizon; and (5) there is indication of potential free gas beneath them. The exception to criterion 2 is the high relief BSR—because these tend to occur along inclined BGHSZ around salt diapirs, they are not parallel to the seafloor.

A model BGHSZ (based on equations from Milkov and Sassen [2001]) was calculated in Fortran using Newton's method and imported into Kingdom Suite software as a grid. Because gas hydrates are not always solely composed of methane (i.e., 100% methane), Milkov and Sassen (2001) provide three equations to calculate the BGHSZ, based on assumed varying concentrations of methane 100%, 95.9%, and 90.4%, with 100% having the thinnest gas hydrate stability zone (GHSZ) and 90.4% having the thickest. The two extremes were plotted to define the region to search for potential locations of BSRs. Although the actual composition of gas is unknown, most natural gas is overwhelmingly methane, so we think BSRs are unlikely to be outside these limits. Thus, BSRs were not interpreted significantly shallower than the pure methane model or significantly deeper than the 90.4% methane model. Exceptions were made in areas of shallow salt due to the model BGHSZ cutting through these salt bodies. The BGHSZ is assumed to be above these salt bodies and our search was adjusted accordingly. The BGHSZ equations from Milkov and Sassen (2001) assumed an approximate geothermal gradient for the Gulf of Mexico that ranged from 15–20° C/km (43–58°F/mi) for deepwater sediments to above 30°C/km (87°F/mi) for shallow water sediments, values similar to those suggested by Nagihara (2006). This approximate geothermal gradient model is empirical and was based on stations (Epp et al., 1970) away from salt bodies (Milkov and Sassen, 2001). With a higher thermal gradient, the predicted BGHSZ would be shallower and with a lower thermal gradient, the predicted BGHSZ would be deeper. Petersen and Lerche (1996) observed that shallow salt exhibits thermal conductivity that is two to three times higher than that of the surrounding sedimentary rocks. This leads to an elevated thermal anomaly above salt features, which Petersen and Lerche (1996) suggested could exceed 30°C/km (87°F/mi) depending upon the geometry of the salt body and the depth of emplacement. Ruppel et al. (2005) found geothermal gradients near fluid expulsion features that are more than ten times background values.

To judge the variability of the geotherm, ~40 heat flow stations were examined in our study area, (proprietary data provided by TDI-Brooks International (TDI-BI). These data stations were loaded into Kingdom Suite and compared with the depth to TOS to note patterns of thermal gradient and to see if there was a correlation between depths to TOS versus thermal conductivity. TDI-BI used a heat flow probe that has a thin (0.236 to 0.393 in [6 to 10 mm]), long (9 to 21 ft [3 to 7 m]) metal tube containing thermistors (typically called a "violin-bow" heat flow probe). This instrument is lowered to the seafloor where it penetrates the
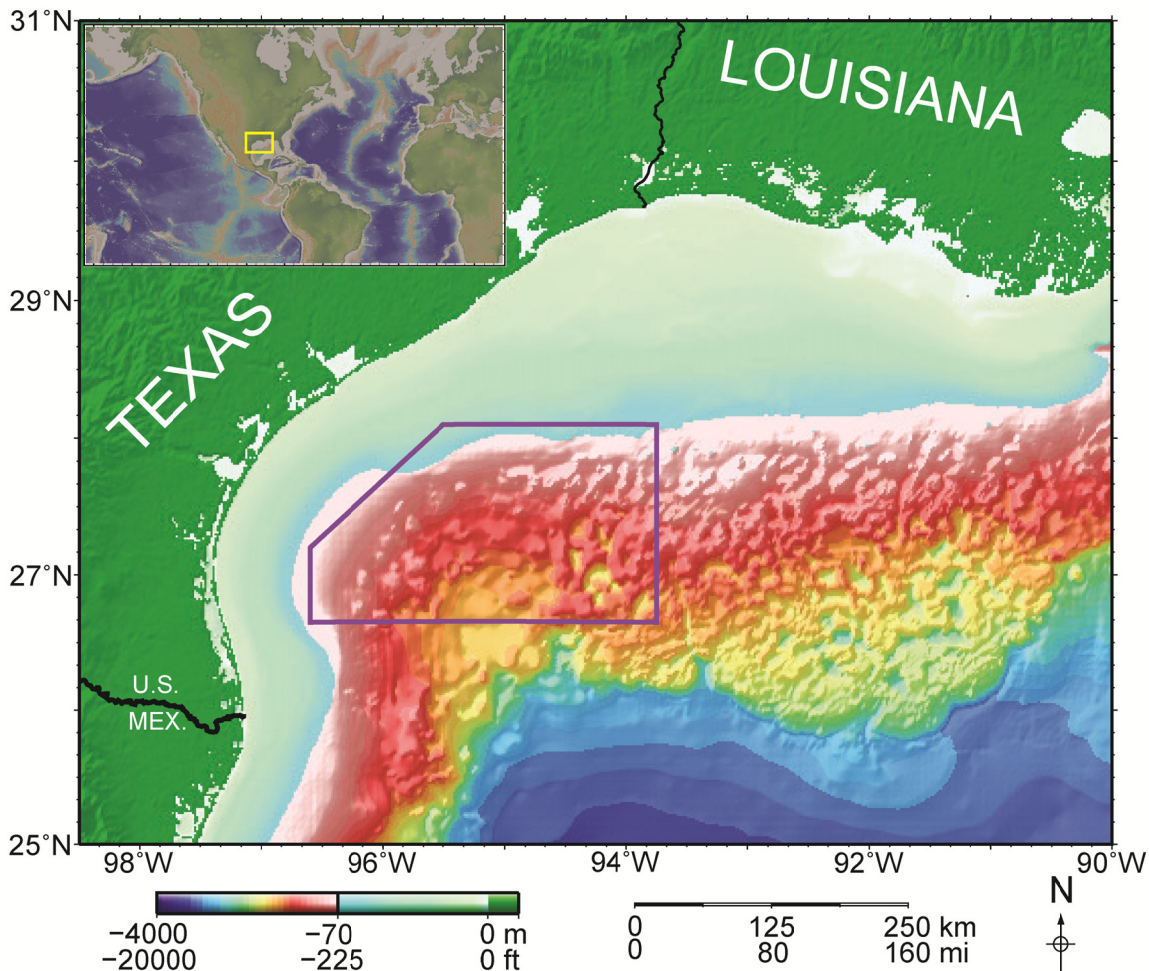
Figure 1. Map of northwest Gulf of Mexico bathymetry, with the survey area outlined. Inset shows location of Gulf of Mexico relative to globe (bathymetry from Smith and Sandwell, 1997).

sediment, measures temperature at different depths and measures in-situ thermal conductivity that then yields the thermal gradient (Nagihara, 2006). Because Nagihara and Smith (2008) concluded there was a significant variation of well temperatures (~30–60°C/km [87–174°F/mi]) along the northwest Gulf of Mexico continental shelf, we would expect to find similar temperature variations on the upper slope as well. Nagihara et al. (1992) showed there was at least a doubling effect of heat flow values related to the tops of salt bodies, thus the TDI-BI data was used as a comparison for our specific study area.

The top of an anomalous, complex sedimentary structure was also mapped. It is a thick, diapiric, gassy sediment package (DGSP). The DGSP top was mapped at the top of chaotic acoustic zones that did not exhibit at their surface a strong seismic reflection or acoustic ringing typical of the TOS horizon.

RESULTS

Top of Salt

The top of salt (TOS) horizon was observed extensively within the study area. The TOS was found to be in the range from 0.65–6.7 s TWTT beneath the sea surface (Fig. 3), the latter value being the maximum vertical extent of the seismic data. The TOS map shows a transition from a broadly continuous canopy punctuated with mini-basins on the east and south sides of

the study area to a zone in the northwest with isolated salt bodies. In many of the areas in Figure 3 that are colored blue, it is impossible to tell whether the salt is deeper than the base of the seismic data or simply absent. The wide spacing of seismic lines in the western half of the survey makes it difficult to determine salt morphology with certainty, and due to this wide spacing, the gridding algorithm used to interpolate the TOS may represent the salt geometry incorrectly. Although exact shapes may be uncertain, even with the wide spacing, it is clear that salt bodies are isolated in the northwest.

Salt in the eastern part of the study area forms large areas of canopy and sheet structures similar to those of the Louisiana slope (Fig. 4). Surface topography in this area is more rugged than the western part of the survey area and many highs and lows of bathymetry (Fig. 2) are mirrored in the TOS topography (Fig. 3). The eastern part of the survey contains several deep basins, probably formed by salt withdrawal. The transition between isolated and more-continuous salt bodies occurs gradually across the study area from the southeast corner, where the salt canopy is broadly continuous (Fig. 4), to the center, where large, complex salt bodies are observed, to the west where salt bodies are mostly isolated diapirs, commonly with upturned sediment layers at their edges (Fig. 5). To the eye, the dividing lines between these zones are highly irregular, but appear to have northeast-southwest trends.
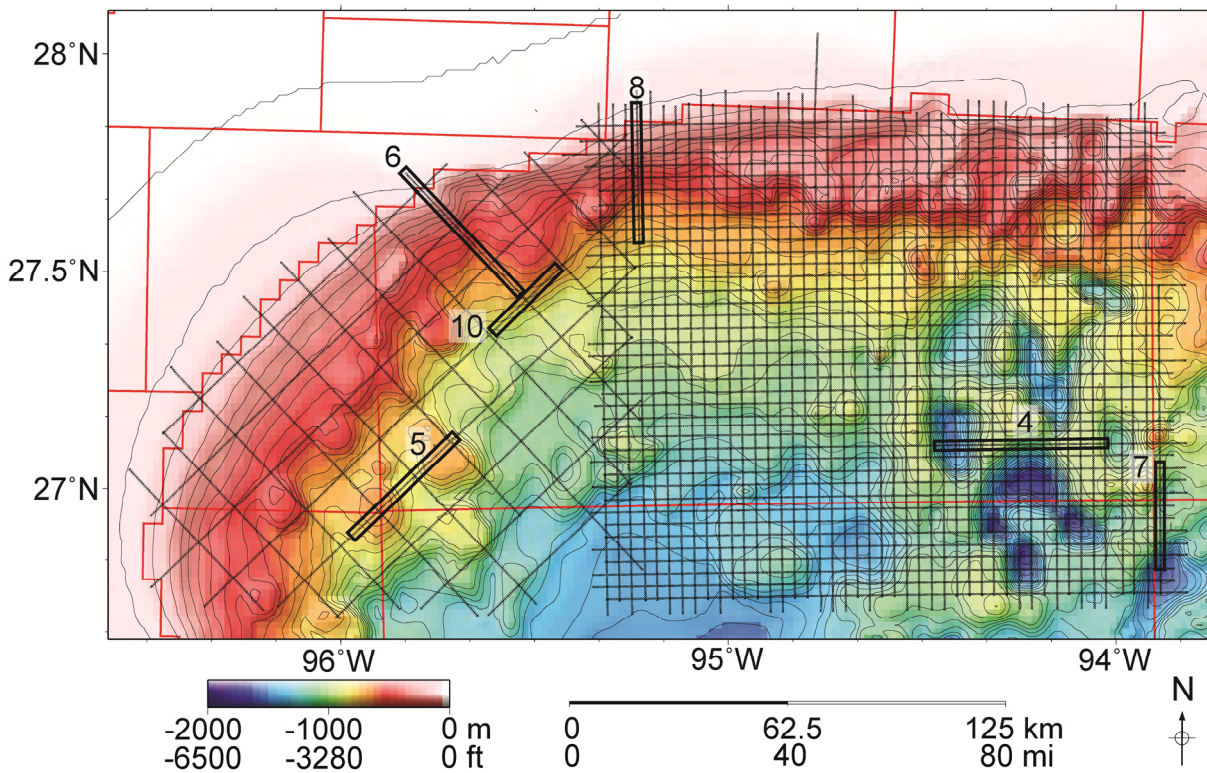
Figure 2. Bathymetric map of the study area with seismic lines superimposed. Numbered line segments are shown in subsequent figures, with numbers denoting figure numbers. Bathymetry contours are shown in 100 m (~330 ft) intervals (bathymetry from Smith and Sandwell, 1997).
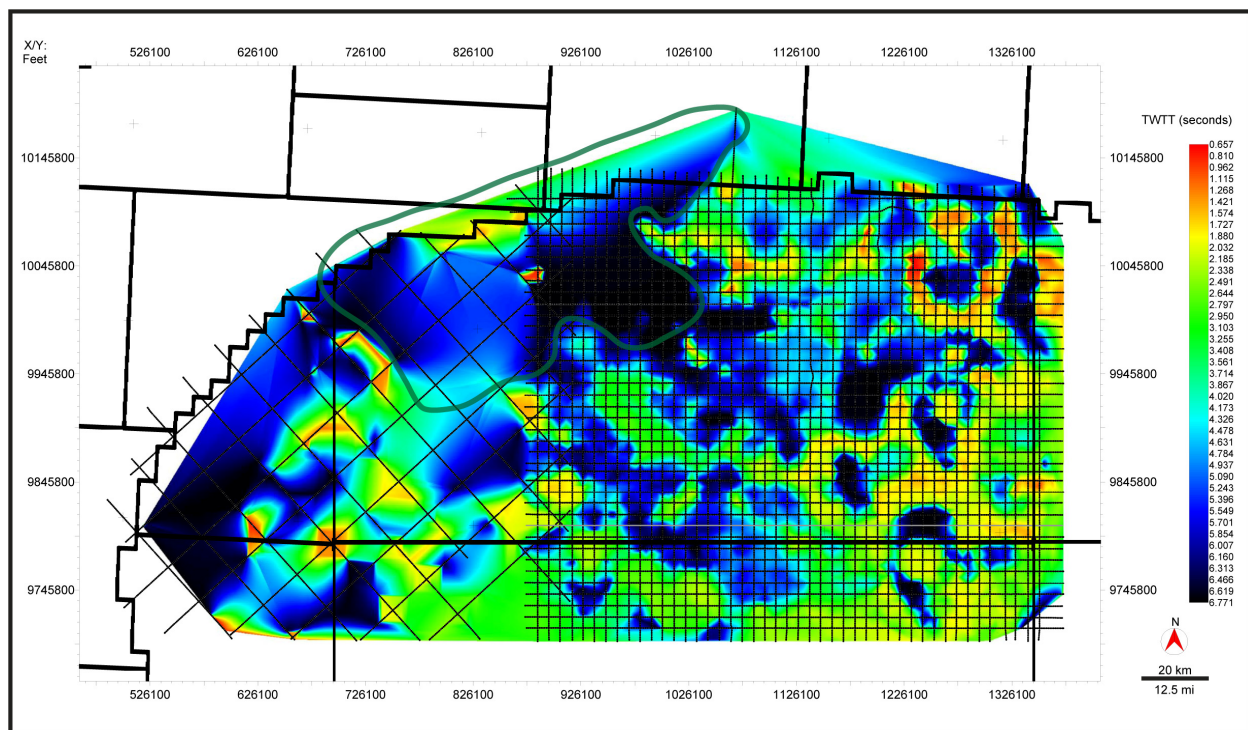

Figure 3. Map of top of salt (TOS). Data are two-way travel time (TWTT) to the top of salt. Warm colors represent shallow TOS and cooler colors show deeper salt. Darker blues indicate no salt or salt is below the base of the seismic data. It is to be noted the gridding algorithm does a poor job indicating in areas where grid spacing is wide, thus cool colors (aqua to dark blue) in the area of widely-spaced tracks and under the DGSP area indicate no salt or salt deeper than the base of the seismic section. Approximate location of the DGSP (see text for explanation) is outlined in green.
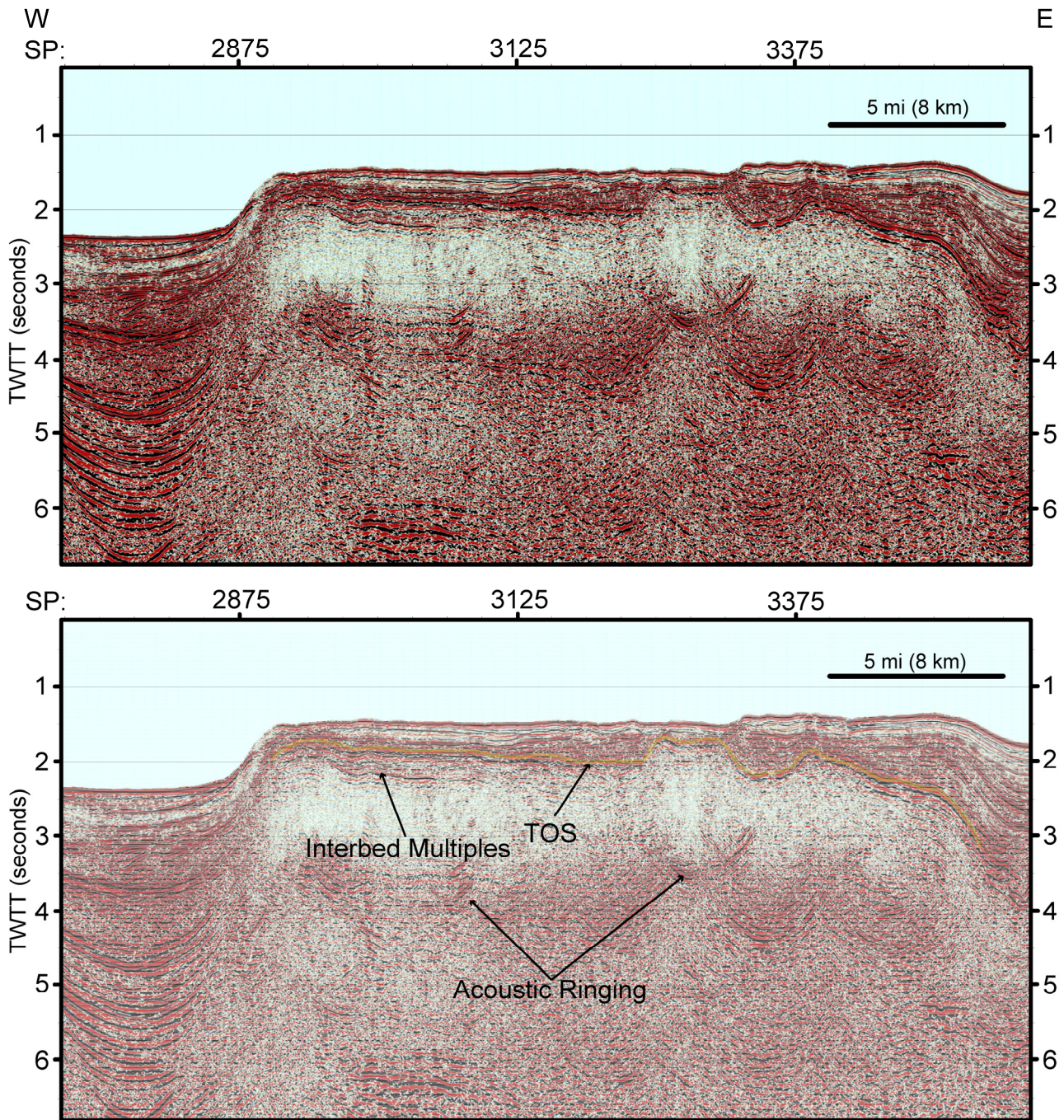
Figure 4. Seismic section showing salt sheet body in the southeast part of the survey area. Examples of interbed multiples are shown as well as acoustic ringing. Vertical scale is in seconds TWTT, and horizontal scale lists shotpoint numbers. Vertical exaggeration is 4:1. Location of section is shown in Figure 2.

The thickness of salt could not be determined with this dataset. The base of salt was not resolvable except in a few areas where the salt is thin. The base of salt is typically poorly imaged or falls below the bottom of the dataset. The TOS creates a large acoustic impedance, thus is easily identified. However, the change in properties from sediment to salt causes reverberation below the TOS and with signal lost at the top interface, it is usually impossible to recognize the bottom of salt.

Faults

Two distinct styles of faulting were observed within the survey area: (1) long, linear normal faults and (2) short, local-ized faults rooted in salt. Faulting styles correlate with salt mor-phology, so they change, from west to east with the style of salt. In the western half of the survey area, faults are long, linear and mostly normal (Fig. 6). They can extend down to nearly the base of the data where they become unresolvable. Regrettably, the coarse spacing of the survey lines does not allow us to correlate the individual faults from one line to the next with certainty. Thus, we cannot determine the exact orientation of the faults in the western area. Though the orientation is unclear, we can still observe an approximate regional trend. The faults are best im-aged on MCS lines trending northwest-southeast (upslope-downslope) and poorly imaged on perpendicular lines, so the faults have trends that are broadly northeast-southwest. This
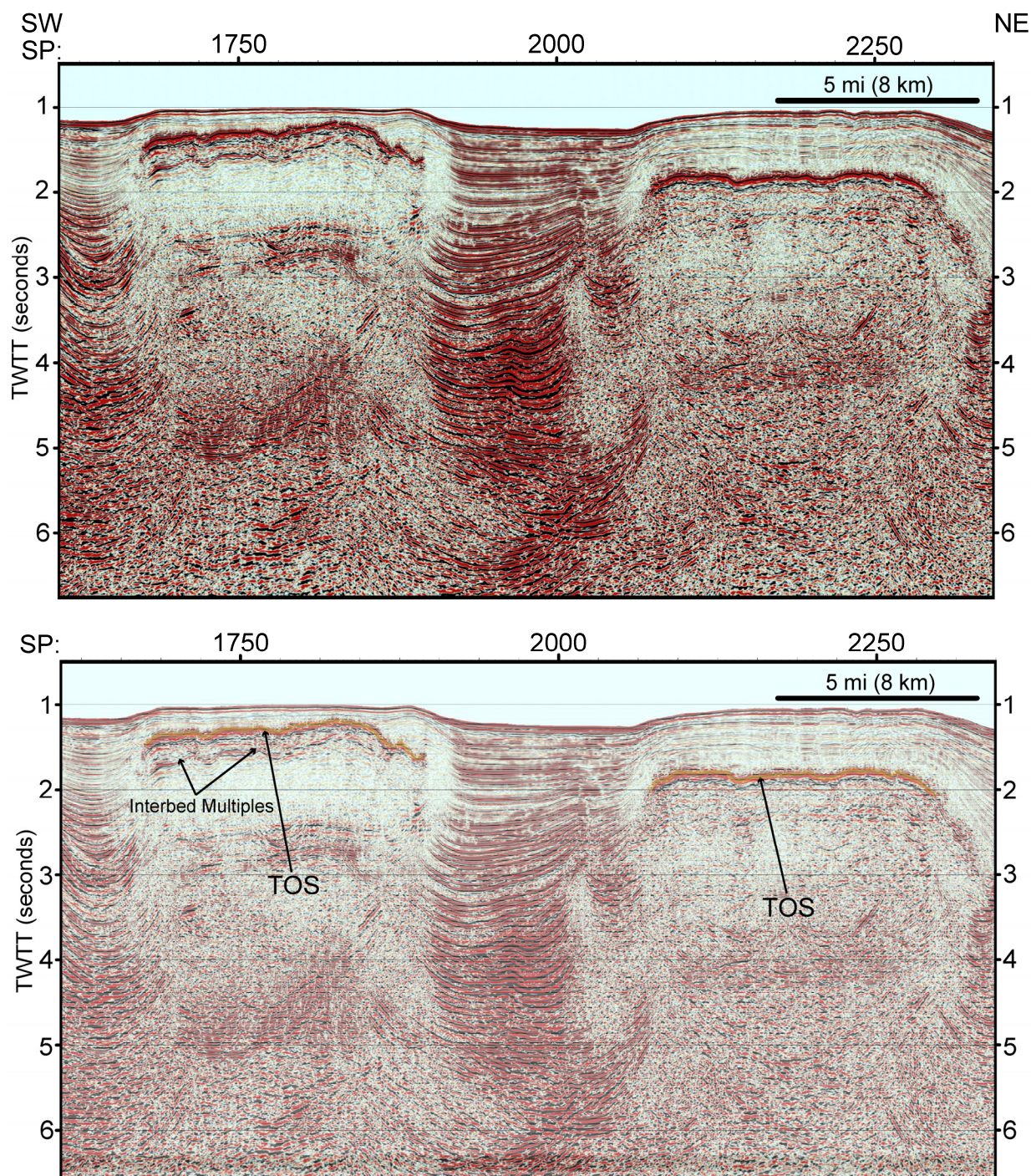
Figure 5. Seismic section showing isolated salt diapirs in the western part of the study area. TOS is indicated by arrows. Vertical scale is in seconds TWTT and horizontal scale lists shotpoint numbers. Vertical exaggeration is 4:1. Location of section is shown in Figure 2.

observation agrees with the definition of regional faults on the Texas slope reported in other studies (e.g., Worrall and Snelson, 1989). The large normal faults typically extend vertically through entire seismic sections indicating deep normal faults. Some of these faults can be seen to offset the seafloor, indicating ongoing activity. The trend and normal nature of the faults implies that they are caused by regional gravitational sliding of the Texas slope sediment wedge (Worrall and Snelson, 1989).

Eastern style faulting is more localized than the regional style faulting in the west. These faults are typically located above the salt sheets and canopies and lie within the shallower sedimen-

tary section (Fig. 7). The faults often root in salt and radiate outward from salt highs, implying a connection with salt body motion. Such faulting is typical of supra-salt faulting caused by local stress fields set up by salt kinematics (Worrall and Snelson, 1989). Both normal and reverse faults can be found, which may indicate salt reactivation and reverse movement on some faults. Offset is common at the seafloor, which is evidence for active salt tectonism (Fig. 7). Although our interpretation is that these faults end at the top of salt, we could not observe faults below the salt. It is likely that they exist, but are disconnected from shallow faults by the intervening salt.
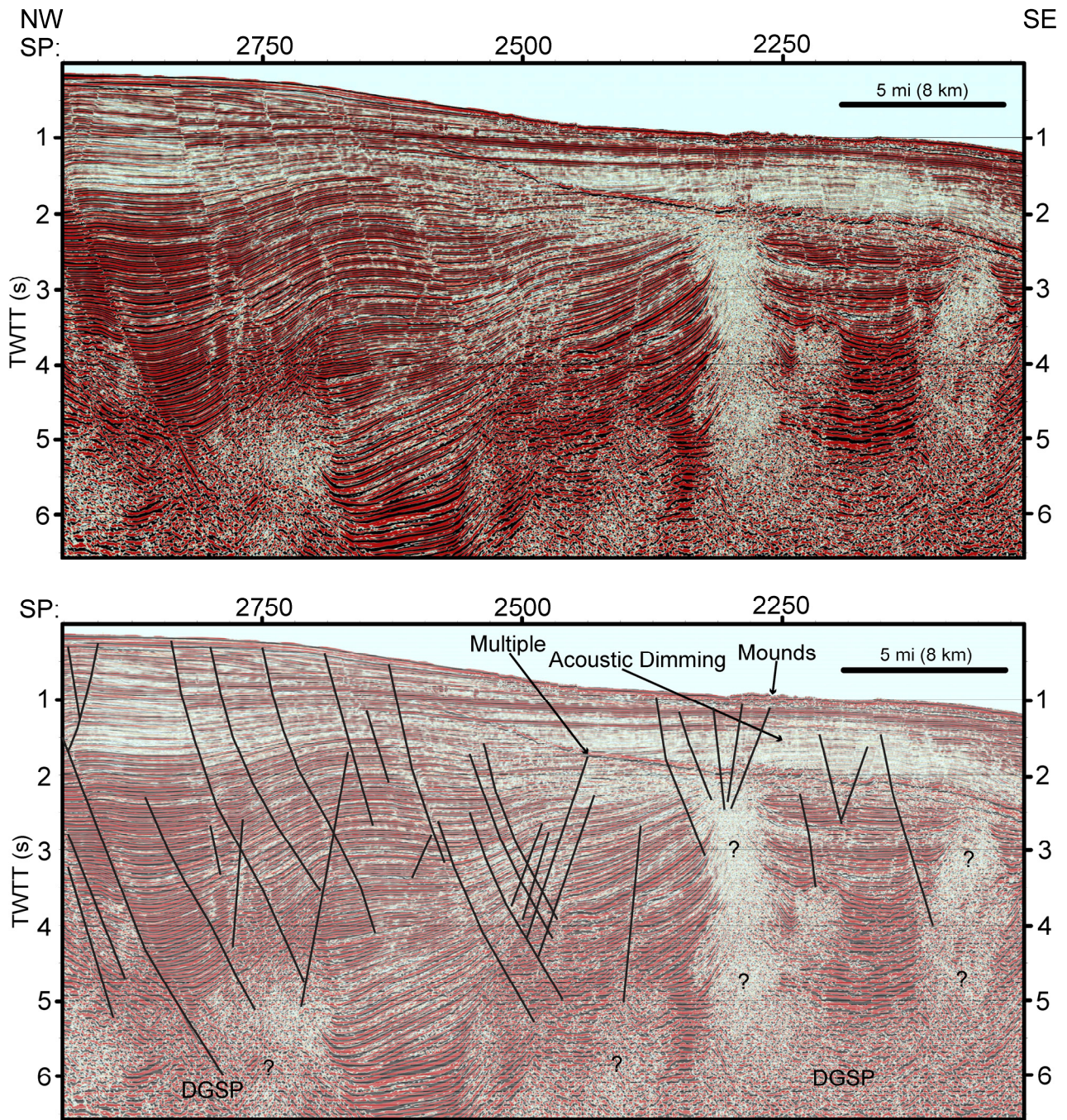
Figure 6. Seismic section showing regional faults produced by gravitational sliding (both regional and counter-regional faults are observed in the plot), vertical gas features (part of DGSP), and acoustic dimming zone. Mounds, a multiple, and acoustic dimming are indicated by arrows. Vertical scale is in seconds TWTT, and horizontal scale lists shotpoint numbers. Vertical exaggeration is 4:1. Location of section is shown in Figure 2.

Gas, Gas Hydrate, and BSRs

There is widespread evidence in the seismic sections of the presence of gas. Gas is evidenced by variations in acoustic impedance that are characterized in several ways: (1) bright spots and layers, (2) ringing, (3) velocity pull down, and (4) areas of acoustic wipeout or dimming. These signatures are widely accepted indicators of free gas, with the different forms resulting from differences in gas concentration, bubble size, and the structure of the sediment (Anderson and Bryant, 1990). Common forms of gas indicator in shallow seismic sections are acoustic

wipeout, dimming (blanking), and acoustic turbidity, all of which give a hazy appearance to the reflectors (Kim et al., 2004). With acoustic wipeout (complete loss of reflections) and dimming (partial loss of reflections), attenuation of seismic reflectors occurs through the portion of the section containing gas. In contrast, acoustic turbidity is an incoherent reverberation in the gas-prone section that causes darkening and masking of subsurface layers. Evidence for both forms can be seen across the entire survey area, typically located above salt bodies or very near the surface. The variation in acoustic wipeout and dimming is a vague indicator to the volume of gas. With decreasing free gas,
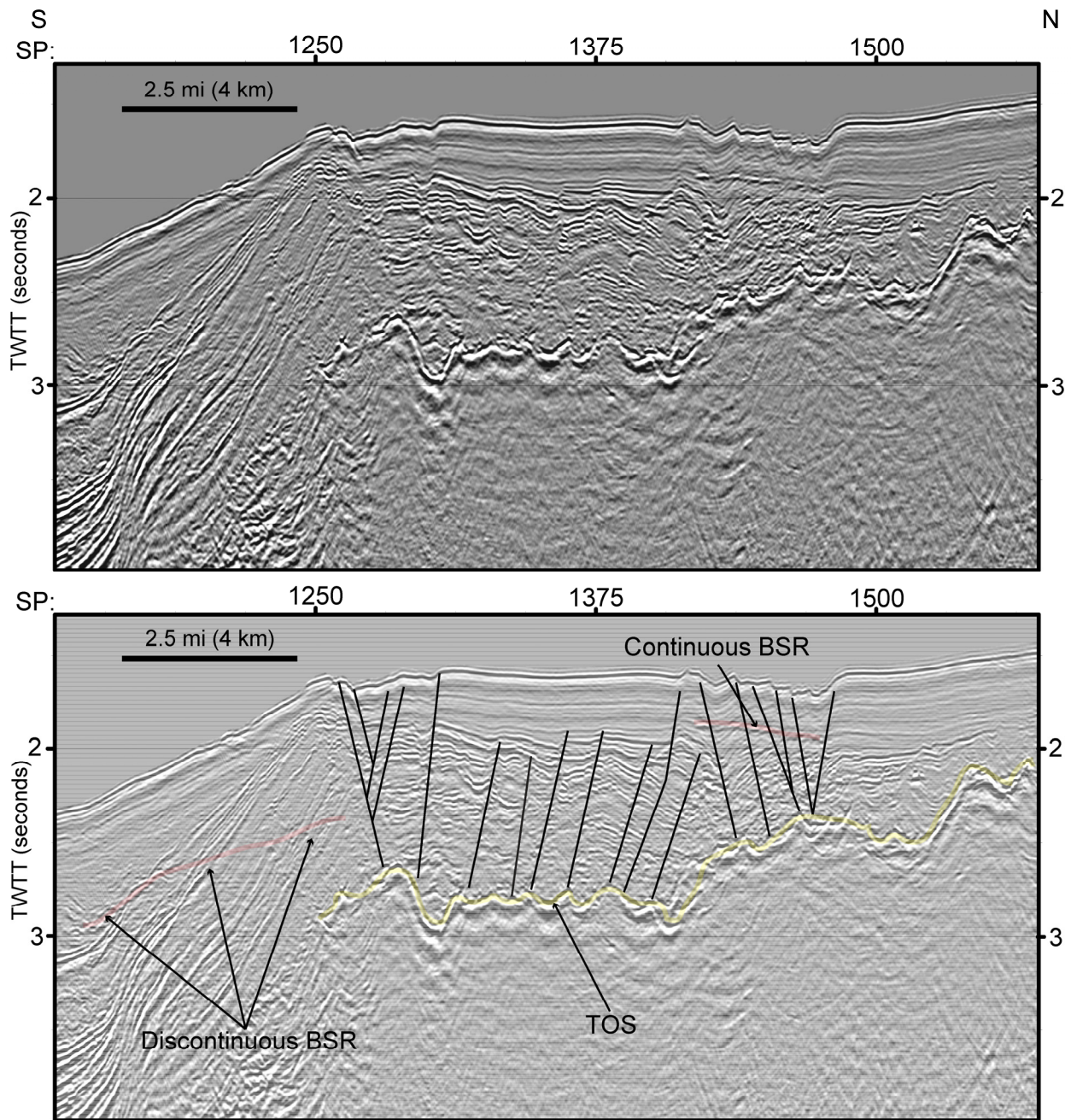
Figure 7. Seismic section showing supra-salt faults characteristic of areas in the eastern part of the survey characterized by the presence of salt canopies and sheets. Two examples of BSR are shown in the plot, one continuous and the other discontinuous. Vertical scale is in seconds TWTT, and horizontal scale lists shotpoint numbers. Vertical exaggeration is 10:1. Location of section is shown in **Figure 2.**

layers become less hazy and more pronounced (Kim et al., 2004). Though free gas trapped beneath gas hydrate can cause acoustic turbidity, we often find acoustic dimming in areas too shallow for gas hydrate formation. An example of slight dimming is shown in Figure 8 at less than 1 s TWTT and shotpoint (SP) 3375. Surface features such as pock marks (Kelley et al., 1994) and mud mounds (Anderson and Bryant, 1990) can lend further support to the interpretation of gas being the cause of acoustic wipeout in seismic sections. Such features are prevalent in our survey area.

In our search for BSRs, we only found one, laterally-limited example of a tcraditional continuous BSR (Fig. 7). We expanded our search to include the non-traditional BSRs as defined by Shedd et al. (2009, 2012) and found many small, laterally-limited

potential candidates (lateral dimensions 0.3 to 9 mi (0.5 to 15 km) (Fig. 9). Most of the candidate BSRs are discontinuous or semi-continuous (i.e., short segments of BSR reflector, often with a larger BSR horizon made up of several short segments). Observed BSRs occur in the central area of the dataset. Few are found in the southeast part, where the salt is more continuous, or in the western area, where the salt volume is low. By eye, there appears to be a correlation between BSR locations and the two northwest-southeast trending areas with deep or absent salt (compare Figures 3 and 9). This correlation probably occurs because BSRs often do not form over shallow salt, unless the salt is thin. The three largest ~9 mi (15 km) BSR candidates were continuous in style, but did not exhibit the cross-cutting relation-

ship with the surrounding beds, thus they could also be explained as gas charged beds. The remaining BSR candidates are smaller and thus difficult to track from one MCS line to another owing to the coarse spacing of the survey. This made lateral mapping of potential BSR candidates difficult. Examples of continuous and discontinuous BSRs are shown in Figure 7.

DGSP

A complex, deep structure was found in the northwest corner of the eastern survey area. This structure, which we term the thick, diapiric, gassy sediment package (DGSP), usually occurs at depths between the base of the seismic section and ~4.5 s TWTT below the sea surface. The package is usually marked by a highly deformed top with overlying sediments that are relatively undisturbed (Figs. 6, 8, and 10). Internally, the DGSP is similar to salt, owing to its diapiric structures and as there is little to no seismic return from within the DGSP. Approximately a dozen tall (~4 s TWTT in height) diapiric structures associated with the top of the DGSP are observed in the survey area. However, the top of the DGSP is not a strong reflector as is the TOS (Figs. 6, 8, and 10). In many cases it is marked by a change from acoustic turbidity to incomplete return of seismic signature (acoustic dimming or wipeout). Often sedimentary layers appear within the attenuated, diapiric zones, commonly having a bowed-upward appearance (Figs. 8 and 10). The base of the DGSP cannot be seen in seismic section due to the depth limitations of the data. The structure of the DGSP is characterized by long (~3–4 km) wavelength folds. In some cases, where the DGSP is found to be in contact with salt, higher frequency folding is observed.

Thermal Gradient

The thermal gradient data were acquired by TDI-BI from scattered locations within the survey area. Measured thermal gradients range from 18–60°C/km (52–174°F/mi) with a mean of ~37°C/km (107°F/mi). Although it is known that the thermal gradient is perturbed by subsurface salt (Nagihara et al., 1992), the data show no strong correlation with salt depth (Fig. 11), indicating other factors, such as salt thickness are also important. The data suggest that the thermal gradient is highly variable and attains high values in places, usually above salt bodies. This complexity is probably a result of complex sedimentary structure, high thermal conductivity of salt, and lateral variations in sedimentation (Hutchinson et al., 2009). The observed large variation in the geotherm implies that the BGHSZ could vary in subseafloor depth by as much as a few hundred meters within the study area. Values higher than the ~30°C/km (87°F/mi) used for our BGHSZ model would push that interface higher in the sediment column.

DISCUSSION

Salt

We observe that the buried salt undergoes a transition from isolated diapirs in the west to a more continuous sheet and canopy in the eastern part of the study area. In the middle part of the study area, we observe diapirs as well as small tongues that are not continuous, but have the appearance of diapirs that have merged together. These observations suggest that the transition is caused by a reduction in salt volume with the result that coalescing diapirs are unable to form a continuous sheet, as occurs further east. Vendeville and Jackson (1992a) and later Rowan

(1995) showed that salt structures in the Gulf of Mexico are dominated by three types of diapirism: (1) reactive (diapirs grow beneath graben), (2) active (diapirs rise by shouldering aside and piercing overburden), and (3) passive diapirism (diapirs originate near the sea floor and grow by downbuilding) with the most common being passive diapirism and the least common being reactive diapirism. Rowan (1995) subdivided passive salt structures into asymmetric and symmetric salt styles and suggested that the difference between passive salt bodies that grow vertically and those that grow asymmetrically to form overhangs may be related to sedimentation rates and patterns. Rowan (1995) further suggested that symmetric salt bodies may have been flanked by fault-bounded depocenters, where high sedimentation rates may have inhibited lateral flow of salt and also found some salt stocks that are cylindrical are related to deep depotroughs.

The western half of the survey area is dominated by sediments and punctuated by isolated salt diapirs. This suggests the original salt deposits were of lesser volume, so that fewer diapirs were formed. The fact that they are isolated and subcircular suggests a radial stress pattern caused by a sediment load that was relatively even. Morton and Galloway (1991) conclude that eustatic sea level was roughly the same throughout the Cenozoic, excepting the Pliocene-Pleistocene, and that sedimentation was relatively consistent. This suggests that sediment loading from the Texas river systems was more-or-less evenly distributed across the slope. This implies the western half of the gulf could be dominated by a passive diapiric or downbuilding regime (Barton, 1933) for its salt structure. Downbuilding occurs when a small dome is created; the salt simply stays in place, always at or near the surface as the sediment is deposited around it and the mother or original salt, subsides (Barton, 1933). The Texas slope salt likely saw evenly distributed hydrostatic pressure, due to the large, even loading of sediments, so it likely formed quasi-symmetric diapirs or simply isolated shallow salt masses. As the diapirs rose, sediments were deposited around them, resulting in continued symmetric growth.

The eastern half of the survey area is characterized by sheet structures and canopy style salt bodies. This area is affected by the distal, fluvial sedimentary load of the Mississippi River system (Worrall and Snelson, 1989; Salvador, 1991). The Louisiana slope region is also the home to the greatest volume of autochthonous Louann salt. As the Mississippi River deposited sediments onto the Louann salt, the sediment loading was uneven, as it avulsed, moving depocenters back-and-forth across the slope. This uneven loading coupled with varying salt thickness led to a more complex salt system due to a varied stress field. As sediments were loaded upon the salt, it was forced to evacuate into shallower sections where its density is in equilibrium, but the main motion was basinward, away from the sediment load. The evacuation of large volumes of salt led to the formation of minibasins, which can be seen in the seafloor bathymetry (Fig. 2). Rowan et al. (2004) suggested that diapir constriction may cause extrusion of allochthonous salt that in turn amalgamates to form a regional canopy.

Faults

Faulting in the western half of the study area consists mostly of long normal faults that often extend down to the base of our seismic sections (Fig. 6). This type of faulting is indicative of gravitational extension (Worrall and Snelson, 1989) and is also characteristic of the Wanda fault system which runs through the northwest part of the survey area (Rowan et al., 2004). Worrall and Snelson (1989) described these faults as "Texas style," be-
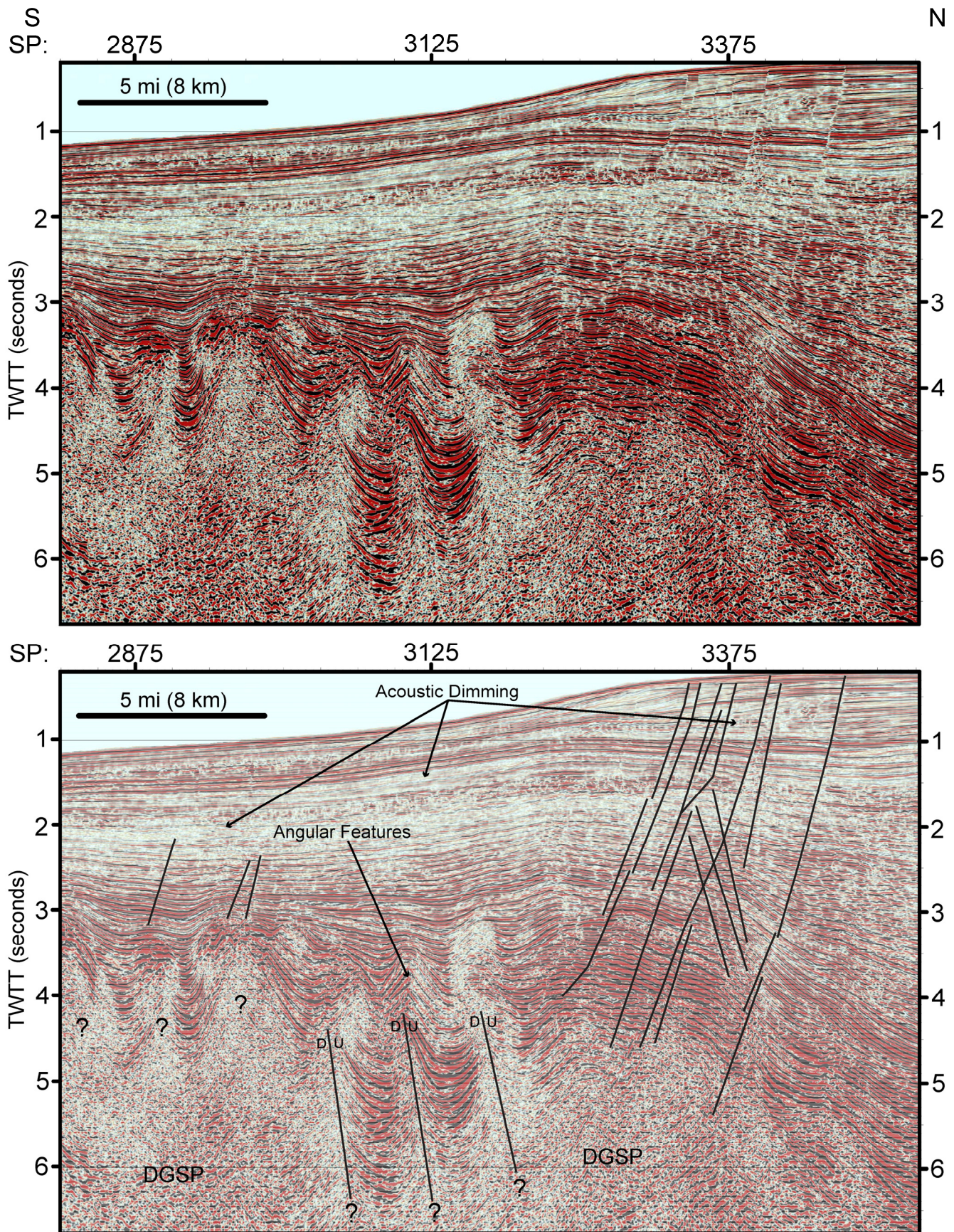
Figure 8. Seismic section showing DGSP. This section of the DGSP has some resolvable bedding that we have interpreted as thrust faults (lower center). U/D symbols indicates upthrown and downthrown blocks, respectively. Some angular bedding is observed. Acoustic dimming (gas indicator) areas are indicated by arrows. Vertical scale is in seconds TWTT, and horizontal scale lists shotpoint numbers. Vertical exaggeration is 4:1. Location of section is shown in Figure 2.
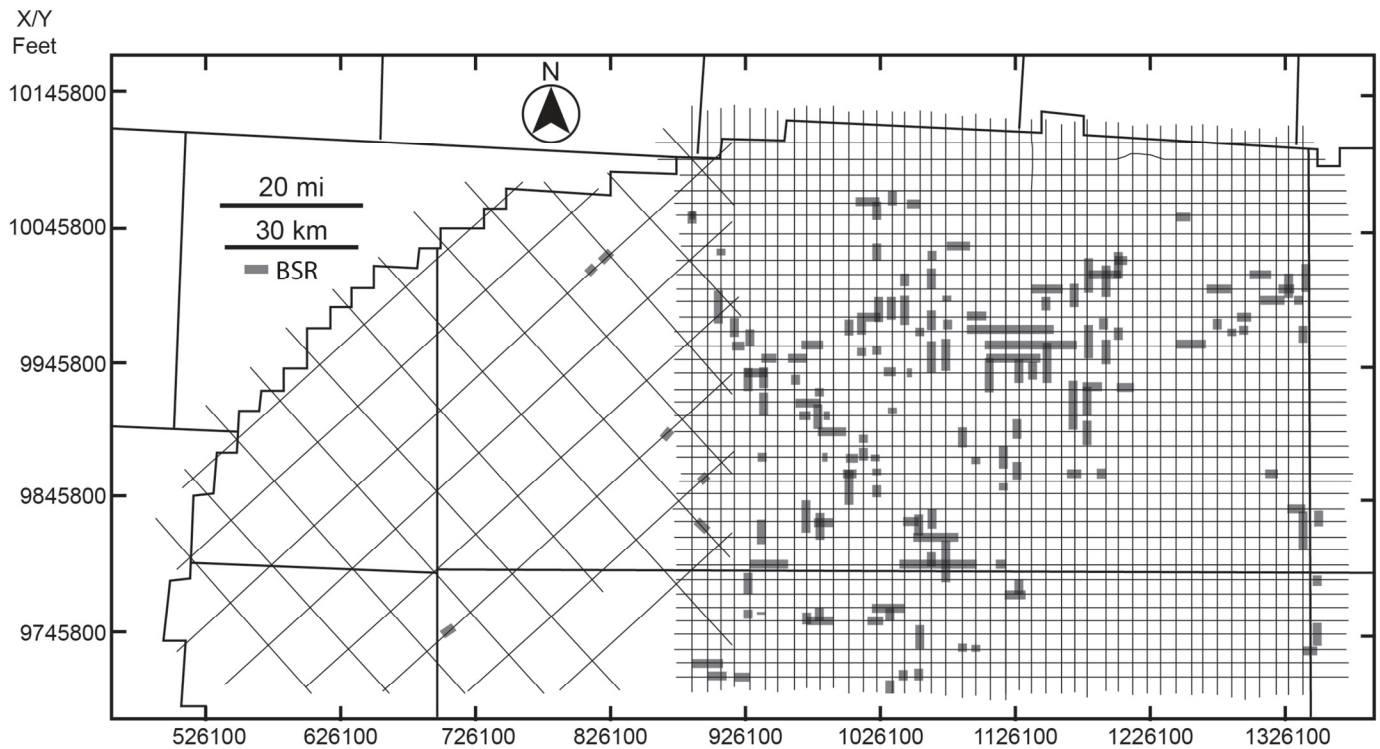
Figure 9. Locations of interpreted BSRs in the study area. Heavy lines show locations where possible BSRs were observed in the seismic sections.

cause they found many similar faults on the Texas shelf and slope. Gravitational sliding occurs because of the massive wedge of sediment on the Texas slope that is not buttressed to the southeast and it slides in that direction. Counter regional faults, long faults that dip towards land, were observed in the western area, but these faults are likely accommodating the movement of sediment and are described as rollover fault families by Rowan et al. (1999). At the base of the section in Figure 6, we observe hazy regions (the DGSP section) into which the Texas faults extend. On approximately a dozen lines, deeper bedding was resolvable and counter-regional faults were observed. The offset in the bedding, however, indicates that they are thrust faults.

Faulting in the remainder of the survey area is mostly the result of mobile salt and is similar in nature to the "Louisiana style" faults of Worrall and Snelson (1989). Continued mobilization of the salt allochthon coupled with continued uneven sedimentation and basin subsidence are major factors behind the current tectonism in the region. Observed faults in the eastern part of the study area are restricted to the thin sediment section above the salt sheets and canopies. Faulting in this region is active as seafloor fault scarps can be seen in the seismic sections, as well as a more rugged TOS topography (Fig. 7). Although we observe faults only above the salt, this is a result of the inability of our seismic data to image sub-salt structures rather than an indication of the absence of faults below the salt.

The difference in dominant fault styles between the eastern and western parts of the study area indicates a significant difference in sedimentation and tectonics. Faults in the eastern half of the survey area are shorter and usually are rooted into a salt surface compared with western styles that extend to the base of the section and likely into a salt weld as suggested by Rowan et al. (2004), or a detachment surface at greater depth (Bruce, 1973; Ewing, 1991; Rowan et al., 2004). Unfortunately, this detachment surface is deeper than the base of the seismic data, thus the

speculation of the fault propagation into this detachment surface is based upon previous work (Bruce, 1973; Ewing, 1991; Rowan et al., 2004). Texas-style faults are produced by a broad regional sediment load whereas the eastern Louisiana-style faults are produced by locally variable stress patterns in a mobile salt dominated regime.

Gas and Gas Hydrate

Traditional BSRs are relatively uncommon in the northwest Gulf of Mexico. In our search, we found only sporadic, limited-extent BSRs (Fig. 8). Either gas hydrate is rare in our study area or we cannot recognize its presence and location easily from low-frequency seismic records because small gas hydrate deposits are beneath the data resolution. Given the widespread occurrence of gas indicators, the latter seems a more likely explanation. Why, then, are BSRs hard to find in the study area?

BSR formation may be inhibited by a number of geological factors including: (1) fluid advection from depth, (2) a highly variable geothermal gradient due to underlying mobile salt bodies, and (3) low porosity and permeability sediments that preclude gas hydrate formation. Both factors 1 and 2 disturb the continuity and geometry of the GHSZ, so if a BSR occurred, it might not have a seafloor-mimicking shape or it might occur at a depth that does not fit the predicted depth from models that assume homogeneous sediments and a constant geotherm. Furthermore, both factors make a portion of the predicted GHSZ inhospitable to gas hydrate. Shedd et al. (2009, 2012) suggested that large, but areally-limited increases in heat flow related to strong vertical fluid flux greatly perturb the BGHSZ. Certainly the heat flow data from the study area indicate large variability in the thermal gradient (Fig. 11). In addition, some of the GHSZ is inhabited by shallow salt, which cannot host gas hydrate owing to its lack of porosity and raises the geotherm, pushing the
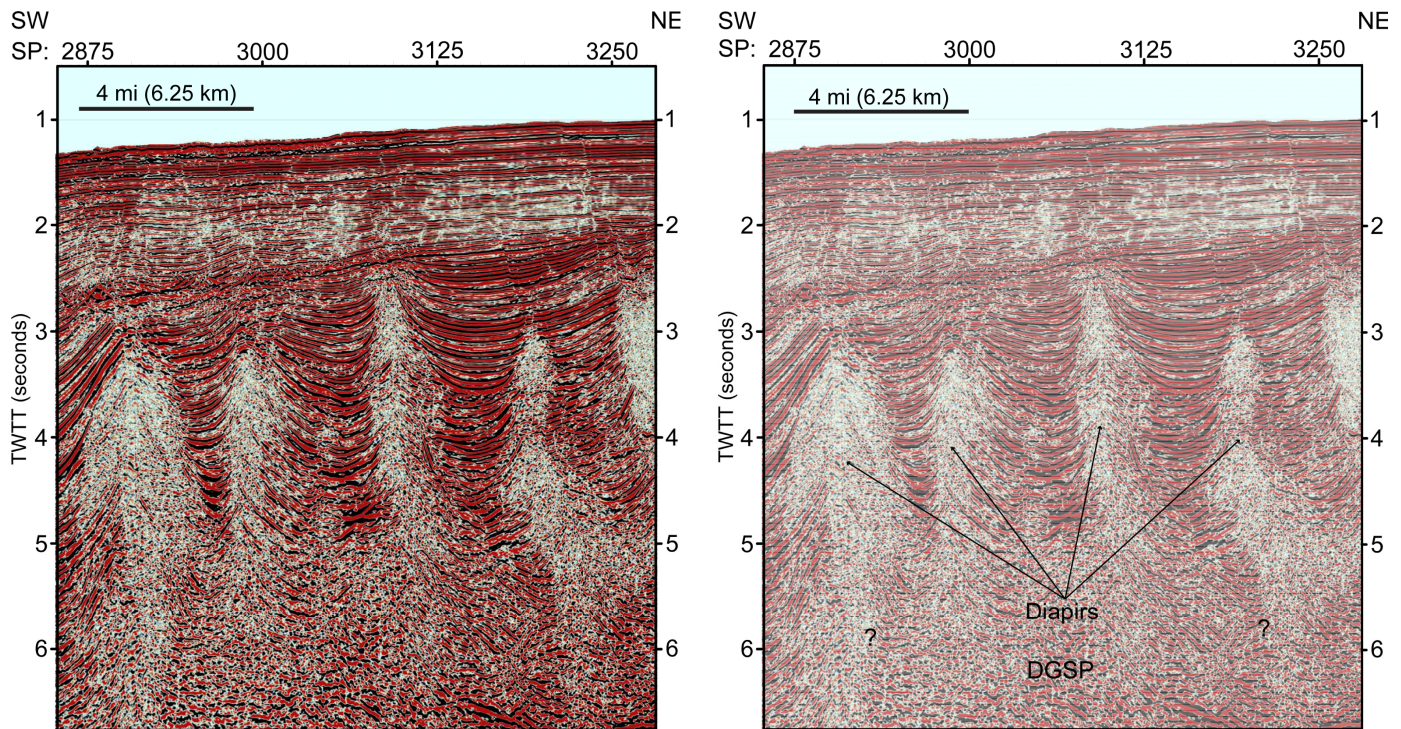
Figure 10. Seismic section showing the DGSP. This section of the DGSP shows the diapir-like structures. Vertical scale is in seconds TWTT, and horizontal scale lists shotpoint numbers. Vertical exaggeration is 4:1. Location of section is shown in Figure 2.

BGHSZ to higher levels. Although these factors could make a BSR into a horizon that does not simply follow the seafloor, they would only rarely make the BSRs go away entirely. Some other factors must be at work.

Factor 3, low porosity and permeability sediment, is important because the ubiquitous clay, silt, and mud sediments in the Gulf of Mexico cannot host significant volumes of continuous gas hydrate deposits owing to the lack of pore space unless they are fractured (Boswell et al., 2012). Even if gas hydrates occur within fractures, those deposits may not be large enough to be recognized by typical exploration seismic data or without special processing (Dai et al., 2008). In the Gulf of Mexico, a significant portion of gas hydrates form within coarse-grained layers that are interspersed within the sediment column (Boswell et al., 2012). If these beds have significant incline, a discontinuous BSR can be recognized where gas turns to gas hydrate across the BGHSZ in each such layer (Fig. 7), making a line of bright spots that follows the BGHSZ (McConnell and Kendall, 2003). Indeed, Shedd et al. (2012) attributed the limited nature of traditional continuous BSRs to the strong lithologic and structural heterogeneity of the northern Gulf of Mexico. Essentially, the BSR reflection only occurs where gas crosses the BGHSZ within sandy (i.e. high porosity and permeability) layers or gas hydrate deposits may be displaced to another part of the GHSZ and thus may not cause an easily-recognized BSR.

This leads to another important observation. In our study area, the layer geometry is also a significant complication. Gas appears prevalent and there are many reflecting horizons with strong impedance contrasts, within, below, and above the GHSZ. Without ground-truth data, we cannot be certain that these reflectors are not caused by strong lithologic contrasts, but it is likely that many bright layers are simply gas-charged, though this is not definitive due to potential velocity inversions, thus well data would confirm the polarity of a particular reflector. In our study

area, sedimentary architecture is complex, but most layers are gently-dipping, so it is difficult to recognize a BSR because it may not cut across strata in seismic sections. Thus, a BSR-like reflector might occur within coarse-grained layers, but we would not recognize it as being the BGHSZ. In our interpretation, we frequently found small segments of reflectors that appeared anomalous, but they were often difficult to trace laterally and frequently blended in with other strong reflectors. Indeed, in many BSRs plotted in Figure 9, the BSR is recognized on one line but not consistently on adjacent or crossing lines. This is attributable to the fact that the BSR is not easily recognized unless the geometry is just right. In addition, if small BSRs exist, they may be below the horizontal resolvability of the low-frequency seismic, and thus would not appear in the seismic data.

It is interesting to compare our mapped BSRs to those reported independently from the study by Shedd et al., (2012). Although Shedd et al. (2012) do not show any examples of BSR on seismic lines within our study area and their BSR map includes our study area at a very small scale, we observe similarities and differences in our interpretations. Shedd et al. (2012; see their Figure 1) show two large patches of BSR (~12–18 m [20–30 km] across) in the middle of the study area and at its southern edge. These appear to correlate to the patches of BSR centered roughly at x/y 1026100–1126100/9745800–9845800 and 1126100–1226100/9945800–10045800. In addition, they report ~12 other small BSR patches (~6 mi [10 km] or less across) in the south central to southeast part of the study area. Our broad-scale pattern of BSR locations (Fig. 9) is similar to that observed by Shedd et al. (2012) in that we see BSRs in the central and eastern part of the study and not in the northern or western parts. In detail, however, it is difficult to see a strong correlation between our individual BSRs and those plotted by Shedd et al. (2012) because the scale of their figure makes it difficult to make one-to-one correlations. Differences in the interpretations proba-
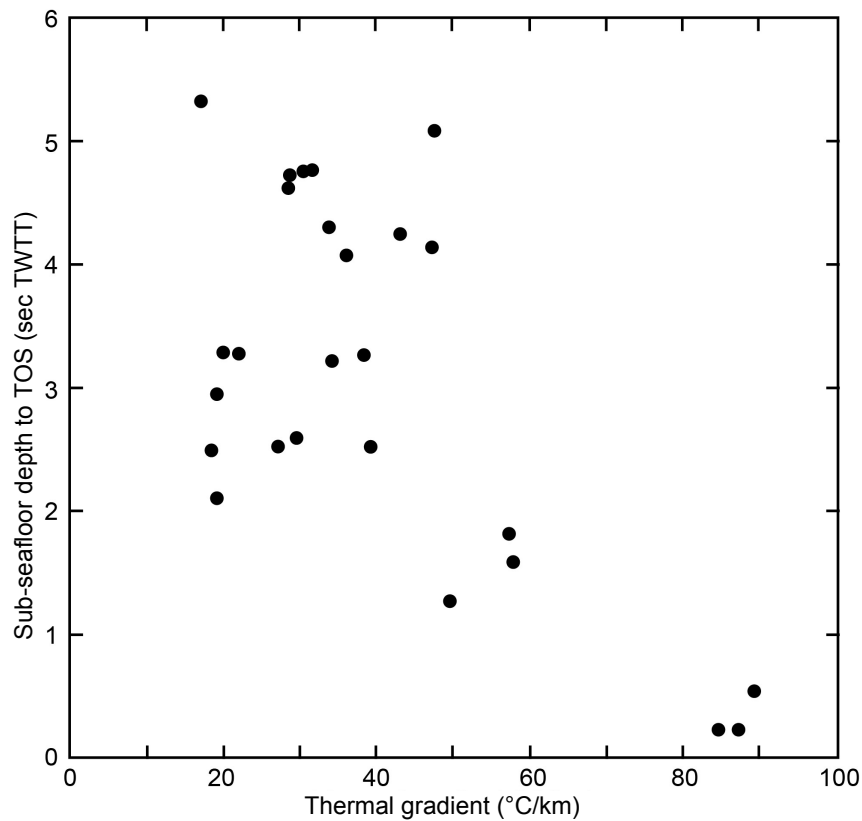
Figure 11. Thermal gradient values measured in the study area plotted versus sub-seafloor depth to the top of salt (in seconds TWTT).

bly occur in part because Shedd et al. (2012) used 3D MCS data, which presumably makes it easier to identify small patches of BSR compared with our widely-spaced seismic lines. The differences, however, also imply that interpretational differences could be significant in the Gulf of Mexico where it is hard to recognize a BSR owing to geologic complexity.

The similarities between our interpretation and that of Shedd et al. (2012) imply geologic control of BSR formation. The two interpretations agree that BSR are rare in the northwest part of the study area. Although this difference appears to be connected to the change from closely-spaced to widely-spaced seismic profiles (Fig. 8), the fact that Shedd et al. (2012) got the same result implies that it is not data dependent. The western area of few BSRs corresponds to the thick wedge of seaward-dipping sedimentary strata that is fractured by Texas-style faults and which has few salt diapirs. Although we do see evidence of subsurface gas in this region, it is not as prevalent as the eastern part of the study, implying that the rest of the study area has more gas to make BSR-like horizons. The dearth of BSRs in the southeast part of the study appears to correlate with the area of nearly-continuous salt canopy and perhaps in this region there is also insufficient gas for widespread BSRs. In the center of the study area, we observe BSR where the sediments are thick, mostly in between salt bodies, implying that deep gas ascends to the near surface in these areas, creating BSRs.

DGSP

The DGSP is a complex structure that is commonly observed in the northwestern part of the study area, particularly in the northwestern corner of the eastern survey area. The DGSP exhibits two frequencies of folding: (1) a broad and gently folded structure (~2.5–3 mi [3–4 km]) with a top punctuated by diapir like structures and (2) a high frequency folding (~0.6–1.2 mi [1–2 km]) that is more commonly found between salt diapirs or against salt bodies. The DGSP is typically marked by an acoustically chaotic zone near large folds with the tops of these folds commonly exhibiting diapiric structure (Figs. 6, 8, and 10). Bruce (1973) and Bishop (1977) found that mobile shales display chaotic acoustic signatures, similar to our DGSP. Carmelo et al. (2004) suggested a similar feature within the northern Port Isabel fold belt was related to the Anahuac shale and that these diapiric features were related to an underpressured mobile shale body, which is unique because diapirism in most shales is thought to be due to overpressure. However, an alternative hypothesis is the DGSP features are related to thrust faulting occurring from an underlying detachment that could be related to mobile shale (Bruce, 1973; Ewing, 1991) or a counter regional salt weld (Rowan et al., 1999). Due to the nature of the diapiric structures associated with the DGSP, as well as nearby large salt bodies that appear to have come from a deeper salt allochthon, and in addition to the different acoustic signature for both salt and salt weld (Rowan et al., 1999), the DGSP is believed to not be associated with a salt weld. Bedding, in some instances, appears to be very tightly folded and angular within and along the sides of the diapir structures, while above the diapir structures a much broader anticline is observed. These features are similar to pop-up structures (Figs. 8 and 10) as described by Camerlo et al. (2004). Camerlo et al. (2004) suggested that similar fold features were related to Anahuac shale diapirism. In some places, bedding is resolvable within a diapiric structure, and bedding offsets suggests thrust faults to be the cause (Fig. 8). The upthrown-downthrown blocks

were determined by observing the overall package of thick sediments between the labeled thrust faults, because the thick package is trending down, while the bedding is stepping up (similar to Rowan et al., 2004). These faults usually extend below the base of our data, which means they could originate from a detachment surface (Rowan et al., 2004). However, in other instances diapiric structures reached almost to the seafloor, as seen in Figure 6, and bedding is not resolvable, suggesting an upward movement gas or a shale diapir.

The DGSP fades eastward and mimics the strike of the Wanda and Corsair fold belts (Worrall and Snelson, 1989) across the region. The nature of the DGSP is difficult to determine with our widely spaced MCS lines. With higher density data, one could better map the top of the DGSP, as well as map the lateral continuity of the diapiric structures. This could help accurately determine whether these are truly diapirs or whether they are some deep rooted counter-regional thrust fault, which in itself may be related to shale diapirism. The Wanda fault system has been mapped to cross roughly through the NW part of our survey area, thus we can infer the folds are likely related to the toe of a major Texas sediment wedge and detachment surface, which would explain the thrust faults (Rowan et al., 2004). Morley (2002) suggested that toe thrust belts are widely associated with deltas on passive margins and also found that the presence of toe thrust belts is a common feature related either to lateral shortening accommodating differential loading by sediments on the shelf or gravity sliding. The change in fold frequency from long to shorter wavelength could be related to salt acting as a "doorstop" of sorts. If there was a large salt body that had been fed by a relatively horizontal salt weld, the salt weld would have acted as a detachment surface. As the sediments continue to slide basinward, sediments above the salt weld could be as ductile as the salt. In this case the salt would not be able to move laterally, thus as the sediments pushed into the salt it would create a doorstop or backstop, similar to an accretionary wedge. This would create a zone of increased differential stresses and could lead to an increase in the number of thrust faults as the stress field attempts to be accommodated at the salt "doorstop" (Rowan et al., 2004).

CONCLUSIONS

The Texas continental slope survey area has two distinct structural styles that allow us to divide it into eastern and western regions based on salt morphology. The western part of the survey is characterized by isolated salt diapirs whereas the eastern part is dominated by salt sheets. The change of salt structure between the two regions is probably the result of original salt deposition and differences in sediment load. The isolated diapirs are formed where original salt deposition was probably thin and where there is a large, even stress field caused by a thick wedge of sediments. The salt sheets of the eastern survey probably result from thicker initial salt bodies, with uneven salt deposition owing to basement graben, and uneven sediment loading from eastern sediment sources. The western area is likely governed by passive downbuilding around salt bodies, whereas the eastern area is dominated by active salt tectonism as indicated by rough topography and numerous fault scarps extending to the seafloor.

Fault styles also change from west to east. Western faults are long, linear and extend through the thick sedimentary wedge, down to the base of the seismic section or into the top of the DGSP. These faults are indicative of extension and a gravity driven sliding of the sediment wedge basinward. Faulting in the eastern region is confined to a thin sedimentary section above

allocthonous salt sheets or canopies. Faulting here is directly related to mobile salt bodies and uneven sediment loading. Salt movement is active as indicated by seafloor fault scarps and is also evident by the rugged TOS.

The DGSP is defined as an acoustically turbid section, with diapiric structures at its top, that displays folding at two frequencies. It could be caused by several different processes, including (1) folded sediments caused by a prograding clastic overburden over a detachment surface, or (2) a mobile shale body, undergoing active diapirism. Without high density seismic data we have limited ability to map its structure and decipher its cause. It is likely that this body is related to the Wanda and Corsair fault systems and may be the toe of a major Texas sediment wedge related to these fault systems. This relationship with the Wanda and Corsair fault systems could explain some of the diapiric structures as thrust faults originating from a deep detachment surface that could be a salt weld or a shale body, but that is impossible to determine with this dataset.

Gas occurs commonly throughout the survey area as indicated by the presence of acoustic wipeout, acoustic turbidity, and bright spots and layers. This suggests there is much gas in sediments on the Texas slope. Nevertheless, we found few examples of BSR, despite the widespread occurrence of gas features, even using expanded definitions of what constitutes a BSR. Our results demonstrate that widespread occurrence of gas is not always associated with discernible BSR features. The lack of BSRs may be related to several geologic factors. (1) Rising warm fluids, specifically brines, likely enter the GHSZ due to many faults reaching the sea floor. This would inhibit the ability of the gas hydrate to form. (2) Higher than normal thermal gradient due to enhancement of thermal conductivity by shallow salt bodies may perturb the GHSZ. These perturbations may cause the BGHSZ to be complex. (3) Widespread low porosity and permeability sediments (i.e., shales versus sands) restrict the porosity within the GHSZ, making gas hydrate deposits conform to bedding and occur at locations other than the BGHSZ. (4) When gas hydrates form within gently dipping sedimentary layers, they will not cause a seismic reflection that will be recognized as a BSR because the BSR will not cross-cut sedimentary layers.

ACKNOWLEDGMENTS

REFERENCES CITED

Anderson, A. L., and W. R. Bryant, 1990, Gassy sediment occurrence and properties: Northern Gulf of Mexico: Geo-Marine Letters, v. 10, p. 209–220.

Barton, D. C., 1933, Mechanics of formation of salt domes with special reference to Gulf Coast salt domes of Texas and Louisiana: American Association of Petroleum Geologists Bulletin, v. 17, p. 1025–1083.

Bishop, R. S., 1977, Shale diapir emplacement in south Texas: Laward and Sherriff examples: Gulf Coast Association of Geological Societies Transactions, v. 27, p. 20–31.

Boswell, R., T. Collett, M. Frye, D. McConnell, W. Shedd, R. Du-

frene, P. Godfriaux, S. Mrowzewski, G. Guerin, and A. Cook, 2009, Gulf of Mexico gas hydrate joint industry project leg II: Technical summary, 26 p. <http://www.netl.doe.gov/technologies/oil-gas/publications/Hydrates/2009Reports/TechSum.pdf> Last Accessed September 12, 2012.

Boswell, R., and T. Collett, T, 2011, Current perspectives on gas hydrate resources: Energy and Environmental Science, v. 4, p. 1206–1215.

Boswell, R., T. S. Collett, M. Frye, W. Shedd, D. R. McConnell, and D. Shelander, 2012, Subsurface gas hydrate in the northern Gulf of Mexico: Marine and Petroleum Geology, v. 34, p. 4–30.

Bruce, C. H., 1973, Pressured shale and related sediment deformation: Mechanism for development of regional contemporaneous faults: American Association of Petroleum Geologists Bulletin, v. 57, p. 878–886.

Bryant, W. R., J. R. Bryant, M. H. Feeley, and G. R. Simmons, 1990, Physiographic and bathymetric characteristics of the continental slope, northwest Gulf of Mexico: Geo-Marine Letters, v. 10, p. 182–199.

Camerlo, R., D. Meyer, and R. E. Meltz, 2004, Shale tectonism in the northern Port Isabel fold belt, *in* P. Post, D. Olson, K. Lyons, S. Palmes, P.Harrison, and N. Rosen, eds., Salt-sediment interactions and hydrocarbon prospectivity: Concepts, applications, and case studies for the 21st century: Proceedings of the 24th Annual Gulf Coast Section of the Society of Economic Mineralogists and Paleontologists Foundation Research Conference, Houston, Texas, p. 817–839.

Dai, J., F. Snyder, D. Gillespie, A. Koesoemadinata, and N. Dutta, 2008, Exploration for gas hydrates in the deepwater, northern Gulf of Mexico: Part I. A seismic approach based on geologic model, inversion, and rock physics principles: Marine and Petroleum Geology, v. 25, p. 830–844.

Dillon, W. P., and C. K. Paull, 1983, Marine gas hydrates—II: Geophysical evidence, *in* J. L. Cox, ed., Natural gas hydrates: properties, occurrences, and recovery: Butterworth Publishers, Boston, Massachusetts, p. 73–90.

Dillon, W. P., D. R. Hutchinson, and R. M. Drury, 1996, Seismic reflection profiles on the Blake Ridge near sites 994, 995, and 997: Proceedings of the Ocean Drilling Program, Initial Reports, v. 164, p. 47–56.

Epp, D., P. J. Grim, and M. G. Langseth, 1970, Heat flow in the Caribbean and Gulf of Mexico: Journal of Geophysical Research, v. 75, no. 29, . 5655–5669.

Ewing, T. E., 1991, Chapter 3: Structural framework:, *in* A. Salvador, ed., The geology of North America, v. J: The Gulf of Mexico basin: Geological Society of America, Boulder, Colorado, p. 31–52.

Frye, M., 2008, Preliminary evaluation of in-place gas hydrate resources: Gulf of Mexico outer continental shelf: Minerals Management Service OCS Report MMS 2008–004, New Orleans, Louisiana, 122 p.

Galloway, W. E., 1989, Genetic stratigraphic sequences in basin analysis II: Application to northwest Gulf of Mexico Cenozoic basin: American Association of Petroleum Geologists Bulletin, v. 73, p. 143–154.

Hornbach, M. J., W. S. Holbrook, A. R. Gorman, K. L. Hackwith, D. Lizarralde, and I. Pecher, 2003, Direct seismic detection of methane hydrate on the Blake Ridge: Geophysics, v. 68, p. 92–100.

Hutchinson, D. R., P. E. Hart, C. D. Ruppel, F. Snyder, and B. Dugan, 2009, Seismic and thermal characterization of a bottom-simulating reflection in the northern Gulf of Mexico, *in* T. Collett, A. Johnson, C. Knapp, and R. Boswell, eds., Natural gas hydrates—Energy resource potential and associated geologic hazards: American Association of Petroleum Geologists Memoir 89, Tulsa, Oklahoma, p. 266–286.

Jones, M. L., S. Nagihara, and M. A. Smith, 2003, The regional geo-

thermal heat flow regime of the north-central Gulf of Mexico continental slope: Gulf Coast Association of Geological Societies Transactions, v. 53, p. 363–373.

Kelley, J. T., S. M. Dickson, D. F. Belknap, W. A. Barnhardt, and M. Henderson, 1994, Giant sea-bed pockmarks: Evidence for gas escape from Belfast Bay, Maine: Geology, v. 22, p. 59–62.

Kim, D. C., G. H. Lee, Y. K. Seo, G. Y. Kim, S. Y. Kim, J. C. Kim, S. C. Park, and R. Wilkens, 2004, Distribution and acoustic characteristics of shallow gas in the Korea strait shelf mud off SE Korea: Marine Georesources and Geotechnology, v. 22, p. 21–31.

Krason, J., P. Finley, and B. Rudloff, 1985, Geological evolution and analysis of confirmed or suspected gas hydrate localities, v. 3: Basin analysis, formation and stability of gas hydrates in the western Gulf of Mexico: U.S. Department of Energy Technical Report DOE/MC/21181–1950, NTIS/DE86001057, Denver, Colorado, 206 p.

Kvenvolden, K. A., 1993, Gas hydrates—Geological perspective and global change: Review of Geophysics, v. 31, p. 173–187.

MacDonald, I. R., N. L. Guinasso, R. Sassen, J. M. Brooks, L. Lee, and K. T. Scott, 1994, Gas hydrate that breaches the sea floor on the continental slope of the Gulf of Mexico: Geology, v. 22, p. 699–702.

MacDonald, I. R., W. W. Sager, and M. B. Peccini, 2003, Gas hydrate and chemosynthetic biota in mounded bathymetry at midslope hydrocarbon seeps: Northern Gulf of Mexico: Marine Geology, v. 198, p. 133–158.

McConnell, D. R., and B. A. Kendall, 2003, Images of the base of gas hydrate stability in the deepwater Gulf of Mexico: Examples of gas hydrate traps in northwest Walker Ridge and implications for successful well planning: The Leading Edge, v. 22, p. 361–367.

Milkov, A. V., and R. Sassen, 2001. Estimate of gas hydrate resource, northwestern Gulf of Mexico continental slope: Marine Geology, v. 179, p. 71–83.

Morley, C. K., 2003, Mobile shale related deformation in large deltas developed on passive and active margins, *in* P. van Rensbergen, R. R. Hillis, A. J. Maltman, and C. K. Morley, eds., Subsurface sediment mobilization: Geological Society Special Publications 216, London, U.K., p. 335–357.

Morton, R. A., and W. E. Galloway, 1991, Depositional, tectonic and eustatic controls on hydrocarbon distribution in divergent margin basins: Cenozoic Gulf of Mexico case history: Marine Geology, v. 102, p. 239–263.

Nagihara, S., J. G. Sclater, L. M. Beckley, E. W. Behrens, and L. A. Lawver, 1992, High heat flow anomalies over salt structures on the Texas continental slope, Gulf of Mexico: Geophysical Research Letters, v. 19, p. 1687–1690.

Nagihara, S., 2006, Pitfalls in marine heat flow probe data acquisition and interpretations: Examples from the Gulf of Mexico: Gulf Coast Association of Geological Societies Transactions, v. 56, p. 643–658.

Nagihara, S., and M. A. Smith, 2008, Regional overview of deep sedimentary thermal gradients of the geopressured zone of the Texas-Louisiana continental shelf: American Association of Petroleum Geologists Bulletin, v. 92, p. 1–14.

Petersen, K., and I. Lerche, 1996, Temperature dependence of thermal anomalies near evolving salt structures: Importance for reducing exploration risk, *in* G. I. Alsop, D. J. Blundell, and I. Davidson, eds., Salt tectonics: Geological Society Special Publications 100, London, U.K., p. 275–290.

Pindell, J. L., 1985, Alleghenian reconstruction and subsequent evolution of the Gulf of Mexico, Bahamas, and Proto-Caribbean: Tectonics, v. 4, p. 1–39.

Ranganathan, V., and J. S. Hanor, 1988, Density-driven groundwater flow near salt domes: Chemical Geology, v. 74, p. 173–188.

Riedel, M., I. Novosel, G. D. Spence, R. D. Hyndman, R. N. Chap-

man, R. C. Solem, and T. Lewis, 2005. Geophysical and geochemical signatures associated with gas-hydrate related venting in the northern Cascadia margin: Geological Society of America Bulletin, v. 118, p. 23–38.

Rowan, M. G., 1995, Structural styles and evolution of allochthonous salt, central Louisiana outer shelf and upper slope, *in* M. P. A. Jackson, D. G. Roberts, and S. Snelson, eds., Salt tectonics: A global perspective: American Association of Petroleum Geologistss Memoir 65, Tulsa, Oklahoma, p. 199–228.

Rowan, M. G., M. P. A. Jackson, and B. D. Trudgill, 1999, Salt-related fault families and fault welds in the northern Gulf of Mexico: American Association of Petroleum Geologists Bulletin, v. 83, p. 1454–1484.

Rowan, M. G., F. J. Peel, and B. C. Vendeville, 2004, Gravity-driven foldbelts on passive margins, *in* K. R. McClay, ed., Thrust tectonics and hydrocarbon systems: American Association of Petroleum Geologists Memoir 82, Tulsa, Oklahoma, p. 157–182.

Ruppel, C., R. Boswell, and E. Jones, 2008, Scientific results from Gulf of Mexico gas hydrates joint industry project leg 1 drilling: Introduction and overview: Marine and Petroleum Geology, v. 25, 819–829.

Ruppel, C., G. R. Dickens, D. G. Castellini, W. Gilhooly, and D. Lizarralde, 2005. Heat and salt inhibition of gas hydrate formation in the northern Gulf of Mexico: Geophysical Research Letters, v. 32, 4 p., doi:10.1029/2004GL021909.

Salvador, A., 1991, Origin and development of the Gulf of Mexico basin, *in* A. Salvador, ed., The geology of North America, v. J: The Gulf of Mexico basin: Geological Society of America, Boulder, Colorado, p. 389–444.

Sawyer, D. S., R. T. Buffler, and R. H. Pilger, Jr., 1991, The crust under the Gulf of Mexico, *in* A. Salvador, ed., The geology of North America, v. J: The Gulf of Mexico basin: Geological

Society of America, Boulder, Colorado, p. 53–72.

Shedd, B., P. Godfriaux, M. Frye, R. Boswell, and D. Hutchinson, 2009, Occurrence and variety in seismic expression of the base of gas hydrate stability in the Gulf of Mexico, USA: Fire in the Ice Methane Hydrate Newsletter, Winter issue, p. 11–14.

Shedd, W., R. Boswell, M. Frye, P. Godfriaux, and K. Kramer, 2012, Occurrence and nature of "bottom simulating reflectors" in the northern Gulf of Mexico: Marine and Petroleum Geology, p. 1–10.

Shipley, T. H., M. H. Houston, R. T. Buffler, F. J. Shaub, K. J. McMillen, J. W. Ladd, and J. L. Worzel, 1979. Seismic evidence for widespread possible gas hydrate horizons on continental slopes and rises: American Association of Petroleum Geologists Bulletin, v. 63, p. 2204–2213.

Smith, W. H. F., and D. T. Sandwell, 1997, Global seafloor topography from satellite altimetry and ship depth soundings: Science, v. 277, p. 1956–1962, ver. 13.1, <http://topex.ucsd.edu/WWW_html/mar_topo.html> Last Accessed January 15, 2012.

Vendeville, B. C., and M. P. A. Jackson, 1991, The rise of diapirs during thin-skinned extension: Marine and Petroleum Geology, 1992, v. 9, p. 331–353.

Watkins, J. S., G. MacRae, and G. R. Simmons, 1995, Bipolar simple-shear rifting responsible for distribution of mega-salt basins in Gulf of Mexico?, *in* C. D. Travis, ed., Salt, sediment and hydrocarbons: Proceedings of the 16th Annual Gulf Coast Section of the Society of Economic Mineralogists and Paleontologists Foundation Conference, Houston, Texas, p. 297–305.

Worrall, D. M., and S. Snelson, 1989, Evolution of the northern Gulf of Mexico, with emphasis on Cenozoic growth faulting and the role of salt, *in* A. W. Bally and A. R. Palmer, eds., The geology of North America, v. A: An overview: Geological Society of America, Boulder, Colorado, p. 97–138.